Authors's last version of the accepted manuscript

Biochim Biophys Acta Biomembr. 2019 Sep 1;1861(9):1579-1591. doi: 10.1016/j.bbamem.2019.07.008. Epub 2019 Jul 10. PubMed PMID: 31301276.

Lidocaine turns the surface charge of biological membranes more positive and changes the permeability of blood-brain barrier culture models

Ana R. Santa-Maria[a,b], Fruzsina R. Walter[a], Sándor Valkai[a], Ana Rita Brás[a], Mária Mészáros[a,c], András Kincses[a,d], Adrián Klepe[a], Diana Gaspar[e], Miguel A. R. B. Castanho[e], László Zimányi[a], András Dér[a]*, Mária A. Deli[a]*

[a]Institute of Biophysics, Biological Research Centre, Hungarian Academy of Sciences, Temesvári krt. 62, H-6726, Szeged, Hungary
[b] Doctoral School of Biology, University of Szeged, Hungary
[c] Doctoral School of Theoretical Medicine, University of Szeged, Hungary
[d] Doctoral School of Multidisciplinary Medical Sciences, University of Szeged, Hungary
[e] Instituto de Medicina Molecular, Faculdade de Medicina da Universidade de Lisboa, Lisboa, Portugal

* Corresponding authors:
Mária A. Deli, E-mail: deli.maria@brc.mta.hu, Tel. +36-62-599602
András Dér, E-mail: der.andras@brc.mta.hu, Tel. +36-62-599606

Abbreviations used:
BI, binary image; bR, Bacteriorhodopsin; CNS, Central Nervous System; BBB, Blood-brain barrier; TJs, Tight Junctions; TEER, Transendothelial Electrical Resistance; DW, Distilled Water; OD, Optical Density; hCMEC/D3, human brain endothelial cell line; RBEC, primary Rat Brain Endothelial Cells; FBS, Fetal Bovine Serum; ITS: insulin-transferrin-sodium selenite medium supplement; MTT, (3-(4,5-dimethylthiazol2-yl)-2,5-diphenyltetrazolium bromide; LDH, Lactate Dehydrogenase; PC-3, human prostate cancer cell line; LY, Lucifer yellow; FD, FITC-dextran; R123, Rhodamine123; AB, apical to basal; BA, basal to apical; PBS, Phosphate Buffered Saline, BSA, Bovine Serum Albumin

Abstract
The surface charge of brain endothelial cells forming the blood-brain barrier (BBB) is highly negative due to phospholipids in the plasma membrane and the glycocalyx. This negative charge is an important element of the defence systems of the BBB. Lidocaine, a cationic and lipophilic molecule which has anaesthetic and antiarrhytmic properties, exerts its actions by interacting with lipid membranes. Lidocaine when administered intravenously acts on vascular endothelial cells, but its direct effect on brain endothelial cells has not yet been studied. Our aim was to measure the effect of lidocaine on the charge of biological membranes and the barrier function of brain endothelial cells. We used the simplified membrane model, the bacteriorhodopsin (bR) containing purple membrane of *Halobacterium salinarum* and culture models of the BBB. We found that lidocaine turns the negative surface charge of purple membrane more positive and restores the function of the proton pump bR.

Lidocaine also changed the zeta potential of brain endothelial cells in the same way. Short-term lidocaine treatment at a 10 μM therapeutically relevant concentration did not cause major BBB barrier dysfunction, substantial change in cell morphology or P-glycoprotein efflux pump inhibition. Lidocaine treatment decreased the flux of a cationic lipophilic molecule across the cell layer, but had no effect on the penetration of hydrophilic neutral or negatively charged markers. Our observations help to understand the biophysical background of the effect of lidocaine on biological membranes and draws the attention to the interaction of cationic drug molecules at the level of the BBB.

Keywords: bacteriorhodopsin, blood-brain barrier, brain endothelial cells, lidocaine, permeability, surface charge

1. Introduction

Every biological membrane shares the same phospholipid bilayer structure, where the hydrophobic fatty acid tail of the phospholipids and the hydrophilic, ionized polar head groups line both surfaces and create the basis of the surface charge of the cell membrane. This surface charge can contribute to the passive or active permeability of ions and metabolites [1,2]. Amphipathic drugs, like many anaesthetics interact with the phospholipid bilayer membranes according to the bilayer couple hypothesis which states that amphipathic drugs affect cells by the asymmetric insertion into one side of the lipid bilayer which increases membrane fluidity [3,4]. Lidocaine is a commercially available tertiary amine used as local anaesthetic. In addition, this lipophilic drug has anti-hyperalgesic, analgesic, anti-inflammatory properties and is also used to treat cardiac arrhythmia [5,6,7]. Lidocaine after being intravenously injected dissociates to a positively charged quaternary amine and to uncharged base forming an in vivo equilibrium between the uncharged and charged molecules, which depends on the local pH [8]. Although the mode of action of local anaesthetics is not fully understood, it is clear that they interact with lipid membranes [9], change the fluidity, micro-viscosity and permeability [8,10]. Hypotheses for the mode of action include that lidocaine might interact with membrane proteins binding to the intracellular site of the voltage-gated sodium channels blocking its action or just inserts to the membrane [9] and interferes with the channel conductivity by changing its shape [8,11,12]. The most accepted theory is that lidocaine inserts to specific binding sites in the membrane, and by its charge blocks the Na^+ current across the cell membrane [11].

Bacteriorhodopsin (bR) is a good simplified model to investigate charge-related changes of biological membranes. bR is a seven transmembrane-helix light driven proton pump with a covalently bound retinal chromophore, found in the cell membrane of *Halobacterium salinarum*, forming purple patches, the so called “purple membrane” [13]. The purple color of the chromophore of bR can be converted to blue, reflecting the inhibition of the proton pump, by two methods: either by removing divalent cations bound to the purple membrane (the “deionized blue” from) [14] or lowering the pH by sulfuric acid solution (the “acid blue” form below pH 3.1-3.2) [15]. The functional bR can be restored either by the addition of cations or raising the pH. It has been shown that cationic lidocaine is able to restore the purple color and the function of the proton pump in deionized bR [16,17], but its effect on acid blue bR has not yet been investigated.

Brain endothelial cells form the morphological basis of the blood-brain barrier (BBB) together with pericytes and glial endfeet, and are key elements in maintaining and regulating

the homeostasis of the central nervous system [18,19]. The most important parts of the physical barrier of the BBB are the interendothelial tight junctions (TJs) and the negative surface charge of brain endothelial cells. This negative charge is derived from the endothelial glycocalyx composed of sialo-glycoconjugates and heparan sulfate proteoglycans [20,21] and the special lipid composition of the plasma membrane of brain endothelial cells [22]. In contrast to other cell types, the negatively charged phosphatidylserine and phosphatidilcholine were the most abundant in endothelial cells from brain [22]. The negative surface charge contributes to the regulation of the permeability for positively charged molecules at the BBB [21,22].

Lidocaine is administered intravenously to treat cardiac arrhythmia [6], therefore it interacts directly with vascular endothelial cells, including brain capillary endothelial cells. According to previous studies lidocaine affects the electrostatic potential of lipid bilayers: the charged molecular form acts at the lipid headgroups, while the uncharged molecule increases the electrostatic potential in the middle of the membrane [23,24]. In the present study our aim was to understand how lidocaine interacts with cell membranes using a simple membrane system containing bR and cell culture models of the BBB. We are the first to study the direct action of lidocaine on the surface charge of brain endothelial cells and their function including electrical resistance and permeability. The endothelial surface charge and its relationship to barrier function is an underresearched area of the BBB field. We hypothesized that lidocaine, a cationic drug molecule, can directly influence the permeability of charged molecules across the BBB.

2. Methods

2.1. Animals

Organ harvest from animals was performed according to the regulations of the 1998. XXVIII. Hungarian law and the EU Directive 2010/63/EU about animal protection and welfare. The local animal health authority, the Governmental Office for Csongrád County, Directorate of Food Chain Safety and Animal Health approved our studies (Permit numbers: XVI/834/2012). For primary cell isolations brain tissues were obtained from 4-week old and 1-day-old Wistar rats (Harlan Laboratories, United Kingdom) of both sexes. Animals were kept under a 12 h light/dark cycle and fed on standard rodent chow and water ad libitum in the conventional animal house of the Biological Research Centre. Following the 3R-rule all efforts were made to minimize animal suffering and pain.

2.2. Materials

All reagents were purchased from Sigma-Aldrich Ltd. Hungary (part of Merck Life Science), unless otherwise indicated.

2.3. Treatments

All treatments performed on bR or *in vitro* cell cultures were done using a stock solution of lidocaine (20 mM, Sigma L7757). Lidocaine was dissolved in water at 30 °C. Stocks were always prepared freshly before each experiment.

2.4. Bacteriorhodopsin assays

2.4.1. Preparation of purple membrane

Purple membranes containing bR were isolated as described previously [13] from *Halobacterium salinarum* strain R_1, which homologously expresses wild type bR and does not tend to form vacuoles, thereby facilitating the isolation procedure. Cultures of *H. salinarum* archaebacteria were grown for about 70-90 h in a shaking incubator, then the culture was centrifuged, pelleted and re-suspended in 200 ml of 25% NaCl solution with 5 mg of DNase. After dialysis against distilled water (DW) the red clear lysate was centrifuged (30 min at 50000 g) and a purple pellet was obtained. To separate the purple membranes from other fragments the pellet was washed once with 4.3 M NaCl, once with 0.1 M NaCl and finally with DW. In the end the purple membrane was centrifuged in a concentration gradient of sucrose from 0.5 to 1.5 M for 10 h at 200000 g in order to remove the red material. From 10 L of bacteria suspension 300-500 mg of purple membrane is gained.

2.4.2. Preparation of polyacrylamide gels

The effects of lidocaine were studied on purple membranes which were immobilized in 0.1% polyacrylamide gel as described previously [25]. Briefly, the gels were prepared using the combination of two solutions. First, tetramethyl-ethylene-diamine (TEMED, Serva, Hungary) was added to the purple membrane suspension with a final dilution of 0.35% (v/v) to prepare the first solution with an optical density (OD) of 4. Then 30% acrylamide/bis mixture (BioRad, Hungary) was prepared containing ammonium persulfate (Serva, Hungary) at a final concentration of 0.1% (v/v). At the end the two solutions were combined and poured into a mould where it polymerized and remained in DW for 24 h.

2.4.3. Treatment of polyacrylamide gels containing purple membrane

Gels containing purple membranes were incubated with different concentrations of lidocaine. For this treatment lidocaine solutions of 10 and 1 mM were prepared in 0.5 mM H_2SO_4 (pH 3.0 - 3.2). The gel slabs (4×4×20 mm in dimension) were soaked in glass flasks containing 15 ml of each treatment solution at 4ºC in the dark for a minimum of 24 h. After the incubation photocycle measurement was performed [26], where a blank gel that did not contain bR was used as a reference. The gel samples were placed in rectangular plastic cuvettes with both the measuring light and the perpendicular exciting laser light crossing through 4 mm pathlengths. The temperature of the samples was kept at 20 ºC during the measurements. Absorption spectra of the samples were taken with a ScanSci miniature spectrophotometer [UNICAM UV/Vis Spectrometer UV4] prior to the photocycle measurement. Time resolved difference spectra after the exciting laser pulse (Continuum Surelight Nd-YAG laser + OPO, appr. 10 ns pulse width) were taken using home built timing and triggering units and an Andor iStar gated CCD detector attached to a Jobin Yvon HR300 spectrograph. The white measuring light from a 35 W Hamamatsu high pressure Xe light source was chopped with a Uniblitz shutter to provide illumination for several tens of milliseconds only during a measuring cycle of 3 s. For the sample in 10 mM lidocaine solution, pH 3.0, 560 nm, for that without lidocaine, at pH 3.0, 630 nm laser pulses were applied in the several 100 μJ range. Difference spectra were measured on a logarithmically equidistant manner from 250 ns to 630 ms with 5 spectra per decade.

2.5. Cell cultures

2.5.1. Blood-brain barrier models

2.5.1.1. hCMEC/D3 human brain endothelial cell line

The human hCMEC/D3 brain endothelial cell line [27] was purchased from Merck Millipore. The cultures of hCMEC/D3 (≤ passage number 35) were grown at 37ºC, 5% CO_2 in MCDB 131 medium (Pan Biotech) supplemented with 5 % fetal bovine serum (FBS), GlutaMAX (100 ×, Life Technologies, USA), lipid supplement (100 ×, Life Technologies, USA), 10 μg/ml ascorbic acid, 550 nM hydrocortisone, 100 μg/ml heparin, 1 ng/ml basic fibroblast growth factor (bFGF, Roche, USA), 5 μg/ml insulin-transferrin-selenium (ITS) supplement (100 ×, PanBiotech, Germany), 10 mM HEPES and gentamycin (50 μg/ml). Medium change was performed every two or three days. When cells reached a confluence of 90% they were passaged for transendothelial electrical resistance (TEER) measurements and permeability assays to rat tail collagen-coated Transwell clear inserts (#3460, 0.4 μM pore size, polyester membrane, Corning Costar), for the zeta measurements to 60 mm Petri dishes (Corning Costar, USA) and for the viability assays to 96-well plates (E-plate, ACEA Biosciences, USA or Corning Costar, USA) Before each experiment the medium was supplemented with 10 mM LiCl for 24 h to improve BBB properties [28].

2.5.1.2. Primary cell cultures

The isolation of primary rat brain endothelial cells (RBEC), glial cells and pericytes and the construction of the *in vitro* BBB model were done according to the method described in our previous studies [29,30]. After isolation, primary brain endothelial cells were seeded on petri dishes (Corning Costar, USA) coated with 100 μg/ml collagen type IV and 100 μg/ml fibronectin in sterile distilled water. The cells were cultured in DMEM/F-12 (Gibco, Life Technologies, USA), 15% plasma derived bovine serum (PDS, First Link, UK), 100 μg/ml heparin, 5 μg/ml insulin, 5 μg/ml transferrin, 5 ng/ml sodium selenite (ITS), 1 ng/ml bFGF (Roche, USA), 10 mM HEPES and 50 μg/ml gentamicin. For the first 3 days of culture 3 μg/ml puromycin was added to the base medium to eliminate P-glycoprotein negative, contaminating cell types [31].

The primary rat brain pericytes were isolated using the same method as described previously, except that pericytes were seeded to uncoated petri dishes (Corning, Costar, USA). Primary cultures of glial cells were prepared from one-day-old Wistar rats and passaged to 12-well plates (Corning, Costar, USA) coated with 100 μg/ml collagen type IV in sterile distilled water. Cultures of rat glial cells were maintained for 2 weeks before using them for the triple co-culture model. The pericytes and glial cells were kept in low glucose DMEM (Gibco, Life Technologies, USA) supplemented with 10% FBS (Gibco, Life Technologies, USA) and 50 μg/ml gentamicin.

The triple co-culture of the primary cells was assembled as described before [29]. Briefly, pericytes at passage number two were seeded at a density of 1.5×10^4 / cm^2 to the bottom of the membranes of Transwell clear cell culture inserts, while RBECs were passaged to the top of the membranes at a number of 7.5×10^4 / cm^2. The inserts were placed into the 12-well plates containing the glial cultures. The triple BBB co-culture model received endothelial culture medium supplemented with 550 nM hydrocortisone and it was cultured together for 4 to 5 days [29]. After the *in vitro* BBB model was established TEER measurements, permeability assays and immunohistochemistry were performed. One day before the permeability assay cells were treated with chlorophenylthio-adenosine-3,5-cyclic monophosphate (250 μM, CPT-cAMP) and phosphodiesterase inhibitor RO 201724 (17.5 μM, Roche) to tighten junctions and elevate resistance [31,32].

2.5.2. PC-3 Human prostate cancer cell line

The PC-3 cell line was purchased from the American Type Culture Collection (ATCC, USA). The cells were cultured in RPMI medium (Gibco), supplemented with 10% FBS and 1% penicillin-streptomycin solution. The cultures were kept in a 10 cm petri dish until reaching 80-90% of confluency, then they were trypsinized and used for the zeta measurements.

2.6. Cell viability assays

2.6.1. Impedance measurement

Kinetics of the viability of brain endothelial cells after lidocaine treatment was monitored by real time impedance measurement (RTCA-SP, ACEA Biosciences, San Diego, CA, USA). Impedance measurement correlates linearly with cell number, adherence, growth and viability [30]. Brain endothelial cells (hCMEC/D3 and RBECs) were seeded at a cell number of 5×10^3 / well onto a 96-well E-plate (ACEA Biosciences) with golden electrodes at the bottom of the wells, and were kept in the CO_2 incubator at 37ºC for 4-5 days, and treated at the beginning of the plateau phase of cell growth with 0, 1, 3, 10, 30, 100, 300 and 1000 µM concentrations of lidocaine. Triton X-100 detergent was used to determine 100% toxicity. Effects of the treatment were followed for 24 h.

2.6.2. MTT and lactate dehydrogenase release assays

For these assays brain endothelial cells (hCMEC/D3 and RBECs) were seeded onto 96-well plates (Corning Costar, USA) at a cell number of 5×10^3 / well. Confluent cultures were treated with 0 - 1000µM of lidocaine or for 30 min, Triton X-100 was used as a 100% cytotoxic control.

Viable cells convert the yellow MTT dye (3-(4,5-dimethylthiazol2-yl)-2,5-diphenyltetrazolium bromide) to purple formazan crystals reflecting metabolic activity. After lidocaine treatment MTT solution (0.5 mg/ml) was added and cells were incubated for 3 h at 37ºC. Formazan crystals produced by living cells were dissolved with dimethyl sulfoxide, and absorbance was measured at 570 nm by a multiwell microplate reader (Fluostar Optima, BMG Labtechnologies, Germany). Cytotoxicity was calculated as a percentage of the control where the maximum dye conversion was detected.

In order, to investigate membrane damage the presence of intracellular lactate dehydrogenase (LDH) enzyme was determined from the supernatant using a commercially available kit [33]. After treatment, culture supernatants (50 µl) were collected into another 96-well plate and were incubated with equal amounts of reaction mixture for 15 min on a horizontal shaker according to the manufacturer's protocol (Cytotoxicity detection kit LDH, Roche). Enzyme reaction was stopped with 0.1 M of HCl and absorbance was measured at 450 nm wavelength using a multiwell microplate reader (Fluostar Optima, BMG Labtechnologies, Germany). Cytotoxicity was calculated as a percentage of the total LDH release from cells treated with 1% Triton X-100 detergent.

2.7. Zeta potential measurements

The zeta potential (ζ) was measured by dynamic light scattering using a Zetasizer Nano ZS instrument (Malvern, UK) equipped with a He-Ne laser ($\lambda = 632.8$ nm). The zeta-potential of the samples was measured at 25 ºC, from a minimum of 6 measurements (maximum 100 runs each), with an applied 20 or 40 V voltage, using disposable zeta potential cells with gold-coated platinum electrodes (DTS1070, Malvern, UK) [22]. Before measurements the zeta cuvettes were activated once with 100% ethanol and rinsed twice with

distilled water. After activation, the zeta cuvettes were calibrated with the zeta standard solution (Malvern, UK) as described in the manufacturer's protocol. For purple membrane samples, the zeta potential measurements were performed at OD=0.1 diluted in 0.5 mM sulfuric acid. Treatment of purple membrane samples was performed with 10 mM lidocaine for 30 min. Cuvettes were always rinsed twice with distilled water between measurements. The hCMEC/D3 and RBEC brain endothelial cells, and PC-3 human prostate cancer cells were used for zeta measurements after cultures reached 90% confluency. Trypsinization of the cells was performed very quickly to minimize plasma membrane changes. After trypsinization, 10^5 cells were re-suspended in 1 ml of PBS with Ca^{2+} and Mg^{2+}. Cells were treated with different concentrations of lidocaine (10, 100 and 1000 μM) for 30 min before the measurement at 37 ºC. The Zetasizer Software v.7.12. calculated the zeta potential values using the Smoluchowski equation [34]:

$$\zeta = \frac{4\pi\mu\eta}{\varepsilon}$$

where μ represents the electrophoretic mobility, η the viscosity of the solvent and ε the dielectric constant.

2.8. Evaluation of barrier integrity

2.8.1. Transendothelial electrical resistance

The BBB models (hCMEC/D3 and the primary cell based co-culture) prepared on inserts received fresh culture medium every second day. To follow the development of the barrier properties of the brain endothelial monolayers TEER was measured before every medium change with an EVOM voltohmmeter (World Precision Instruments Inc., USA) combined with STX-2 electrodes. TEER was expressed relative to the surface of the inserts ($\Omega \times cm^2$). The TEER of cell-free inserts (100 $\Omega \times cm^2$) was subtracted from the measured values. TEER before and after lidocaine treatment was measured in Ringer-Hepes buffer supplemented with 1 % BSA and ITS. This buffer had the same composition as used for the permeability measurements. To decrease fluctuations in the TEER due to temperature change measurements were performed by placing the culture plates to a heating pad set to 37 °C.

2.8.2. *Permeability measurement with marker molecules of different surface charge*

Permeability tests on the BBB models on inserts were performed when TEER values reached previously published values (86±9, n=24 for D3, 255±15 for RBEC n=24 co-culture; [35], showing the barrier properties for both models. For the permeability experiments inserts were transferred to 12-well plates containing 1.5 ml Ringer-HEPES buffer (118 mM NaCl, 4.8 mM KCl, 2.5 mM $CaCl_2$, 1.2 mM $MgSO_4$, 5.5 mM D-glucose, 10 mM HEPES, pH 7.4) supplemented with 1 % BSA and ITS in the lower (basal/abluminal) compartment. In the upper (apical/luminal) compartment culture medium was replaced with 0.5 ml buffer containing 10 μM lidocaine and molecular markers with different surface charges: FITC-dextran (10 μg/ml, FD, Mw: 10 kDa) with neutral charge, positively charged rhodamine123 (10 μM, R123, Mw: 380 Da) and negatively charged Lucifer yellow (5 μM, LY, Mw: 457 Da). Cells serving as control were only incubated with the fluorescent markers without any lidocaine treatment. The plates were kept in a CO_2 incubator at 37 °C on a horizontal shaker (150 rpm) for 30 min. After incubation the samples were collected from the compartments and the concentrations of the marker molecules were determined by a spectrofluorometer (Horiba Jobin Yvon Fluorolog 3, Kyoto, Japan). Excitation/emission

values for the different markers were: 440 nm/516 nm for FD; 498 nm/525 nm for R123; 420 nm/535 nm for LY.

Transendothelial permeability coefficient (P_e) was calculated as previously described [29,30]. Briefly, clearance was calculated from the transport of the fluorescent marker molecule from the donor to the acceptor compartment expressed as µl of donor compartment volume from which the tracer was completely cleared. The average cleared volume was plotted vs. time, and permeability surface area product value for endothelial monolayer (PS_e) was calculated by the following formula:

$$\frac{1}{PS_{endothelia}} = \frac{1}{PS_{total}} - \frac{1}{PS_{insert}}$$

PSe was normalized for the surface area of the Transwell insert (1.12 cm^2) and was expressed as 10^{-6} cm/s. In measurements from the apical to basal (AB) direction the upper compartment served as the donor and the lower compartment as the acceptor. In the case of the basal to apical (BA) direction the donor compartment was the lower, while the acceptor compartment was the upper one.

2.8.3. Immunohistochemistry

After the permeability assays brain endothelial cells were stained for junctional associated proteins β-catenin and ZO-1 and for tight junction protein claudin-5 to assess the morphological changes after lidocaine treatment. Cells were fixed with cold acetone-methanol solution (1:1) for 2 min, washed with phosphate buffered saline (PBS) and non-specific binding sites were blocked with 3% bovine serum albumin (BSA) in PBS for 1 h at room temperature. Incubation with primary antibodies (dilution 1:200) polyclonal rabbit anti-β-catenin (Sigma C2206), polyclonal rabbit anti-ZO-1 (Invitrogen, 61-7300) and polyclonal rabbit anti-claudin-5 (Sigma, SAB4502981) lasted overnight at 4 ºC. The next day cells were incubated with anti-rabbit secondary antibody labeled with Cy3 (Sigma C2306; dilution 1:400), and bis-benzimide H33342 (Merck, Germany) to stain nuclei, for 1 h at room temperature. Between incubations cells were washed three times with PBS. Stainings were visualized by a Leica TCS SP5 confocal laser scanning microscope (Leica Microsystems, Germany). Pictures for the junctional-cytoplasm intensity ratio evaluations were taken with the exact same settings among cell types and stainings.

2.9. Image analysis

The fluorescently labeled images were analysed using Matlab software (R2019a, MathWorks, Inc.). In brain endothelial cells the fluorescent intensity of the immunostaining for junctional proteins in the cell membrane is higher than in the cytoplasm. First we determined the cytoplasmic intensity, from which binary images (BIs) were created. The complementary BIs were considered as the junctional staining in the plasma membrane. The pixels in the two BIs were used as masks, and the intensities of the original pixels were summed in both the junctional BIs and the cytoplasmic BIs separately. The ratio of the cell membrane and cytoplasm intensities for each image was determined and used for the statistical analysis. The number of images were 11-15 in each group.

2.10. Measurement of efflux pump activity

The activity of the P-glycoprotein efflux pump was measured by R123, a ligand of this transporter, similarly to the permeability assay, but both in the AB and BA directions.

For measurements in the BA direction the donor compartment was the lower, while the acceptor compartment was the upper one. As a reference Pgp pump inhibitor, cyclosporin A (10μM) was used (30 min pre-treatment of cells). During the assay cells were incubated for 30 min with 10 μM R123 with or without 10 μM lidocaine in Ringer-HEPES buffer. After the incubation samples were collected from the upper and lower compartments and the concentration of R123 in the samples was determined by a spectrofluorometer (Horiba Jobin Yvon Fluorolog 3; excitation/emission: 498/525 nm).

2.11. Statistics

Data are presented as means ± SD. Statistical significance between treatment groups was determined using t-test, one-way or two-way ANOVA followed by Dunnett or Bonferroni multiple comparison post-tests (GraphPad Prism 5.0; GraphPad Software, USA). All experiments were repeated at least twice, and the number of parallel samples was minimum three. Changes were considered statistically significant at $p < 0.05$.

3. Results

3.1. Effect of lidocaine on the purple membranes

The chromophore of the bR is sensitive to the absence of divalent cations bound to the purple membrane at neutral pH: upon removal of divalent cations by deionizing the membrane suspension, the color of bR changes from purple to blue, which is accompanied by inactivation of the proton pump [14]. Purple membrane also turns blue, and the proton pump is inhibited in sulfuric acid solution with pH below 3.1-3.2 [15]. This condition is shown on Fig. 1A when no lidocaine treatment is present and the gels containing purple membrane turn blue due to the acidic pH. Lidocaine treatment at 1 and 10 mM concentrations reversed this color change (Fig. 1A), an effect that was concentration dependent.

Fig. 1B shows the absolute spectra of the samples with and without 10 mM lidocaine treatment at pH 3.0. As observed also visually, the sample without lidocaine was blue (pure blue) as expected at this pH due to the protonation of the proton acceptor Asp85 already in the resting state of the pigment. The sample treated with 10 mM lidocaine at pH 3.0 turned purple. The absorption spectrum of the latter has a maximum close to the position expected at neutral pH, whereas that of the blue membrane is substantially red shifted. As both spectra appeared wider than the spectrum of bR at higher pH, we estimate that both are mixtures of the pure purple and pure blue forms. An estimate of 25/75% and 75/25% contribution of the purple and blue forms to the zero and the 10 mM lidocaine samples, respectively, yields narrower calculated spectra of the two pure forms (Fig. 1B). Representative time resolved difference spectra measured on the purple membrane containing gel samples at pH 3.0, with and without 10 mM lidocaine treatment, are shown in Fig. 1C and D. The purple samples in 10 mM lidocaine display a regular photocycle typical at higher pH with consecutive L, M and O intermediates, with characteristic absorption peaks seen at 6.3 μs after excitation at 410 nm (L); 400 μs, 410 nm (M) and 16 ms, 640 nm (O), followed by the recovery of the initial bR state in about 100 ms. The amount of accumulated O in the 10-100 ms range is relatively high as expected for the "normal" photocycle below the pK_a=5.8 of the proton release cluster[37], where proton release is delayed to the very end of the cycle, coinciding with the decay of the O intermediate. On the other hand, the photocycle without lidocaine is characteristic of the truncated cycle of the blue membrane. Here M does not accumulate since the proton acceptor Asp85 is already initially protonated so that the Shiff base cannot

deprotonate. After the accumulation of a small amount of L-like intermediate the photocycle terminates faster than in the case of the purple membrane.

3.2. Modulation of surface charge of purple membranes

Due to the absence of a direct measurement for the surface charge, to evaluate the electrostatic properties of membrane surface, zeta potential can be determined [22]. We measured the zeta potential of purple membranes in 0.5 mM sulfuric acid and found it highly negative (-36.4 ± 0.4 mV, Fig. 2). Lidocaine treatment for 30 min changed this value to more positive (-21.9 ± 0.3 mV), indicating a direct action of the cationic drug on the charge of membranes containing bR. This shift in the charge can explain the changes we observed in the purple membrane color (Fig. 1A) and the shift in the bR spectrum (Fig. 1B).

3.3. Effect of lidocaine on cell viability in the BBB models

First, the effect of lidocaine on the viability, metabolic activity and membrane integrity was studied using the hCMEC/D3 cell line and primary RBECs. Lidocaine at 1–300 μM concentrations did not cause any drop in the cell impedance after 30 min (Fig. 3A-B). At the 1000 μM lidocaine treatment concentration impedance decreased after 30 min, but this decrease was temporary, reversible and cells recovered to the viability level of the control within 2 h.

Incubation of the cell monolayers for 30 min with lidocaine in the concentration range of 1-1000 μM did not cause any alteration in the metabolic activity of the cells indicating no cell damage by the MTT conversion assay (Fig. 3C-D). To determine if lidocaine damages the plasma membrane integrity LDH assay was performed. As shown in Fig. 3E-F, the release of LDH from the brain endothelial cells did not increase compared to the control. Triton X-100 detergent was used as a reference compound to elicit 100% toxicity in all the assays (Fig. 3).

3.4. Lidocaine as a modulator of surface charge in living mammalian cells

We hypothesized that lidocaine can change the surface charge of biological membranes which was confirmed in our measurements of zeta potential of purple membranes. To further investigate this phenomenon, we tested the effects of lidocaine on the zeta potential of living mammalian cells. In this study we used single cell suspensions from the hCMEC/D3 human brain endothelial cell line, primary RBECs and the PC-3 prostate cancer cell line with or without 10, 100 and 1000 μM lidocaine treatment. The base zeta potential for all three cells types was negative, -11.4 ± 1.3 mV for the hCMEC/D3 cells (Fig. 4A); -12.3 ± 1.2 mV for the RBECs (Fig. 4B) and -20.1 ± 0.9 mV for the PC-3 cell line (Fig. 4C). Since lidocaine is metabolized very quickly in the body by the liver, we chose the 30 min treatment window. The background zeta values became more positive after treatment with increasing lidocaine concentrations in the case of all three cell types (Fig. 4) proving that lidocaine interferes with the surface charge of living cells as well.

3.5. Integrity of the BBB models after lidocaine treatment

In clinical patients toxic side effects were only seen above 5 μg/ml (21.7 μM) plasma concentration of lidocaine [38]. To use a clinically relevant, but not toxic concentration of lidocaine, we selected the 10 μM for the barrier experiments.

The BBB restricts the movement of not only cells and large molecules, but also ions [32]. The most common method to determine the tightness of the barrier is to measure the

TEER. Therefore, to investigate the effect of lidocaine on the barrier properties of the BBB models we first measured resistance. There was a three times difference between the TEER values of the BBB models showing that the primary co-culture model better restrict the movement ions as compared to the simplified BBB model (Fig. 5A-B). Lidocaine treatment (10 μM, 30 min) decreased the TEER on both models. The TEER drop in hCMEC/D3 cells was 35% (84±6 to 55±10 $\Omega \times cm^2$) while on the triple co-culture BBB model it was only 17% (252±19 to 211±6 $\Omega \times cm^2$).

Since lidocaine modified the surface charge of biological membranes, we hypothesized that the permeability of charged molecules across the BBB models might also change. We used three differently charged fluorescent markers to determine their permeability across brain endothelial cells after lidocaine treatment. In the hCMEC/D3 cell line model the permeability for the water soluble negatively charged marker LY and neutral marker FD did not change as compared to the control group but the cationic molecule R123 showed an increased flux after lidocaine treatment (Fig. 5C). For the primary BBB co-culture model (Fig. 5D), also no change was observed for the LY and FD, although the P_{app} values of the markers were much smaller (LY: 1/10, FD: 1/3 of the P_{app} in hCMEC/D3 model) showing once more that the integrity of the barrier is stronger in the co-culture model. As compared to the cell line model the permeability of the cationic marker, R123, decreased after lidocaine treatment (Fig. 5D). This result is in accordance with our hypothesis, which presumes that the interference of lidocaine with the membrane charge decreases the permeability of a lipophilic cationic marker across the BBB if the paracellular pathway is closed.

To confirm the effects of lidocaine on brain endothelial barrier integrity, immunostainings were performed for junctional proteins β-catenin, ZO-1 and claudin-5 (Fig. 6A-B). We evaluated the subcellular expression of junctional proteins after lidocaine treatment with fluorescent intensity measurements (Fig. 6C-D). In the control groups of both BBB models the immunostainings were mainly located at the cell borders, where the cell junctions are found. RBECs showed elongated morphology with close cell-cell contacts (Fig. 6B). After 10 μM lidocaine treatment a slight morphology change was visible in both models. The β-catenin showed a cytoplasmic rearrangement both in the hCMEC/D3 and the RBEC models. Similar change was observed for ZO-1 in the hCMEC/D3 cells. Claudin-5 was not detectable in this cell line (see Fig. S1 in Supplementary material). RBEC showed a redistribution of the claudin-5 tight junction protein after lidocaine treatment which is also reflected by the modest TEER decrease (Fig. 5).

3.6. Lidocaine is not an efflux pump blocker

Since R123 is not only a positively charged lipophilic compound, but also a ligand of the Pgp efflux pump, we wanted to further investigate, whether lidocaine interferes with the activity of the Pgp function. Bidirectional permeability assay was performed, which showed that cyclosporin A by blocking Pgp increased the R123 flux in AB direction and decreased it in the opposite direction across the primary cell based BBB model (Fig. 7). In contrast, lidocaine treatment (10 μM, 30 min) decreased the permeability of R123 across RBECs from the AB direction and did not change the flux from the BA direction, indicating that lidocaine does not inhibit the activity of the Pgp efflux pump.

4. Discussion

The BBB has special defense systems constituted by the TJs, the efflux pumps and the metabolic enzymes of brain endothelial cells [19,39]. This line of defense is strengthened by the negative surface charge of brain endothelial cells which regulates the entrance of charged molecules through the BBB [21,40,41], but this area is not extensively studied. In our experiments we investigated the effects of lidocaine on the surface charge of brain endothelial cells, which gets into the systemic circulation as an antiarrhythmic drug [6], and can have a direct effect on the vascular system. Previous *in vivo* studies have shown that lidocaine protects the BBB in high blood pressure caused barrier opening [42] or in peripheral nerve damage [43]. However, its effect on the surface charge and the barrier properties of brain microvessel endothelial cells have not yet been described. This study is the first to reveal the direct effects of lidocaine on the surface charge of biological membranes and its effects on the permeability of BBB models contributing to a wider knowledge on the interaction of cationic molecules at the level of BBB. To generalize the effects on surface charge and function, in addition to the hCMEC/D3 human brain endothelial cell line and a primary rat brain endothelial cell based culture models we also used purple membrane as a simple membrane system. According to our hypothesis, lidocaine can influence the surface charge of the brain endothelial cell membrane and by this it can also affect BBB function.

4.1. The effect of lidocaine on purple membranes as a simple model system

The lipid content in the isolated purple membrane is about 25%. Sulphated glycolipids are exclusively found in the purple membrane, and they are responsible for the negative charge [44]. Lidocaine treatment for 30 min had a direct action on the bR: a shift in both the purple membrane charge and the bR spectrum occurred (Fig. 1A and Fig. 1B). The blue color of the gels containing purple membrane was triggered by the low pH that also inhibits bR function (Fig. 1A). When the pH is low, the large amount of protons compensate the negative surface charge of purple membranes and provoke protonation of a crucial side chain of bR stopping its pumping action [15]. When lidocaine is added, it substitutes protons at the membrane surface, and allows bR to function again. The absorption spectrum and the photocycle of bR at pH 3.0 were typical for the acid blue membrane [13]. This result is similar to previous observations on deionized bR, where the deactivation of the proton pump was achieved at pH 7 by the removal of the divalent metal ions bound to the membrane, and the effect was reversed by cationic amine anaesthetics, including lidocaine [17]. Note, however, that in the latter caser purple color can be restored by any other common cations as well [14]. Based on the zeta potential measurements and the spectral data one can conclude that lidocaine acts as a local factor increasing the pH close to the membrane surface by at least 1-2 units, thereby affecting the protonation state of even buried residues of the protein. The decay of O intermediate, that coincides with the recovery of the initial state is nevertheless substantially slower than the recovery at neutral pH, indicating that this step involves the direct extracellular proton release from Asp85 rather than the internal proton transfer from Asp85 to the proton release cluster. Hence the latter remains protonated during the photocycle as expected at effective pH values below the pK_a=5.8 of the proton release cluster [37].

4.2. The effect of lidocaine on the viability of brain endothelial cells

After we confirmed our hypothesis that lidocaine can influence the surface charge, hence the function, of a simple biological membrane, we were interested in the effects of lidocaine on living cells. Lidocaine is used in the pharmacotherapy as a local anesthetic and

has a clinically important role in the treatment of abnormal heart rhythm [8,38]. When given intravenously, it can act directly on brain endothelial cell membranes and might affect barrier properties of the BBB. To avoid the side effects of lidocaine, such as heart attack or neurologic symptoms, the concentration of the lidocaine treatment should be optimized [38]. The therapeutic plasma concentration of lidocaine is between 1.5 and 5 μg/ml (6.5-22 μM). In order to determine the direct effect of lidocaine on the viability of brain endothelial cells, toxicity tests were performed. No change was seen in any of the assays for the tested concentrations, except for a reversible reduction of the impedance value at the highest, suprapharmacological concentration of 1000 μM (Fig. 3). These data are in accordance with the low toxicity and the safe applicability of lidocaine as a therapeutic drug [6]. Since lidocaine is metabolized by the liver within 2 h and the half-life of the drug is short in the blood [6,38], we selected the clinically relevant 10 μM concentration and the 30-min treatment time to study the surface charge and barrier function of the BBB models.

4.3. The effect of lidocaine on the surface charge of the brain endothelial cells

While the hydrophobic interaction of lidocaine with the lipid bilayer of the cell membrane, including membrane fluidity, and its influence on protein channels has been studied [8,45], our study is the first to measure the effect of this drug on surface charge of living cells. In the vascular system the surface charge of brain endothelial cells is more negative than that of peripheral endothelial cells [22]. This can be explained by the special lipid composition of the plasma membrane of brain microvascular endothelial cells [22] and the denser structure of glycocalyx in the luminal surface of brain capillaries [46]. In concordance with the first measurement of the zeta potential of bovine brain endothelial cell suspension [22], we also found that the surface charge of human and rat brain endothelial cells are negative and in the same range (Fig. 4). Lidocaine treatment, as we measured it on the simple model system, made the zeta values of the cells more positive, indicating a direct effect on the surface charge in both models. The surface charge elevation in mammalian cells after 1 mM lidocaine treatment (~40% from the control) was similar to the bR zeta potential change caused by 10 mM lidocaine. Since treatment of bR purple membranes with the same concentration of lidocaine already resulted in a considerable color change, we suggest a similar effect in both model systems. We have also tested lidocaine on a different type of cell, a human prostate cancer cell line, and found a similar effect. Our data on lidocaine and surface charge is supported by previous findings with a cationic lipid probe, TMA-DPH. This probe, which inserts into the plasma membrane of cells, made the zeta potential of brain endothelial cells also more positive [22]. The role of the surface charge of molecules, especially cationic ones, to cross the BBB has been long known [21], but only recently measured [41]. The positively charged ibuprofen-kyotorphinamide derivative not only increased the zeta potential of brain endothelial cells, but the molecule had an increased analgesic effect in mice indicating higher penetration to brain [41].

4.4. The effect of lidocaine on the barrier function of brain endothelial cells

The BBB restricts the transport of substrates, from ions to large molecules, between the blood and the CNS [19]. The two major pathways for molecules and cells to cross the BBB are the paracellular (junctional) and the transendothelial routes [32,39]. The TJs are important in permeability regulation, because they not only restrict paracellular flux, but also maintain polarity of enzymes and receptors on the luminal and abluminal membrane domains [47]. The measurement of TEER is the most sensitive method to assess the tightness of TJs

in BBB models [32,48]. The resistance of brain endothelial cell layers was slightly, but significantly decreased by lidocaine (Fig. 5A) suggesting an increased paracellular ionic permeability. This change was reflected by the redistribution of the immunostaining for three junctional proteins, β-catenin, ZO-1 and claudin-5 in brain endothelial cells from the plasma membrane to the cytoplasm after lidocaine treatment (Fig. 6A-B) which was quantified by image analysis (Fig. 6C-D).

There was no significant difference between the control and the lidocaine treated groups in the permeability of the negatively charged and hydrophilic markers, LY and FD (Fig. 5C-D). This result indicates that lidocaine treatment affects the paracellular pathway for ions, but not for larger water-soluble molecules (for a more detailed explanation and drawings see Fig. S2 and S3 in Supplementary material). The other marker molecule, R123 is positively charged and lipophilic, therefore it crosses a tight barrier by the transcellular pathway. If the barrier is not tight, R123 is diffusing by both the trans- and the paracellular pathways. On the cell line BBB model the permeability of the R123 after lidocaine treatment was increased (Fig. 5C). This can be explained by the weaker barrier properties and the more dominant paracellular pathway of the hCMEC/D3 cell line as compared to the primary cell based BBB models [28,48], and as we confirmed by the TEER data (Fig. 5A). In the case of the primary brain endothelial cell co-culture model, where TJs are tighter and the paracellular pathway is more closed, as reflected by the several fold higher TEER, the permeability of the cationic R123 was decreased by the positively charged lidocaine (Fig. 5D). We suppose that there can be a physicochemical interaction between lidocaine and R123, two positively charged molecules, at the surface of brain endothelial cells decreasing the transcellular permeability of R123 in the apical to basal direction (Fig. 8). In accordance with our data, lidocaine decreased the permeability of cationic drugs pentazocine and naloxone across the BBB in rats, but influx drug transport systems may participate in the brain uptake of these molecules [49,50]. We cannot exclude the possibility, that other mechanisms than membrane interactions also participate in the effect of lidocaine on BBB permeability.

Since R123 is a ligand of the Pgp efflux pump [29], one of the most important efflux transporter at the BBB [19,48], we studied if lidocaine has an effect on Pgp activity. The action of lidocaine was opposite to cyclosporine A, our reference inhibitor, suggesting that it does not inhibit the Pgp efflux pump (Fig. 8). Inhibition of Pgp did not change brain/plasma concentration of lidocaine in rats [51] indicating that lidocaine does not interact with the efflux pump, in agreement with our finding.

5. Conclusion

Lidocaine, a cationic drug, made the surface charge of biological membranes more positive in simple model membranes and in living mammalian cells. This physical membrane effect restored the proton pump activity at acidic pH in purple membranes and altered the function of endothelial cells forming the barrier protecting the brain. Lidocaine increased the ionic permeability of brain endothelial cell layers, but the paracellular pathway did not change to water-soluble marker molecules. In contrast, the permeability of a cationic lipophilic marker was decreased, suggesting interaction of the cationic molecules at the membrane level. Lidocaine had no effect on the function of the Pgp efflux pump. From these data, we can conclude that lidocaine can change the surface charge, an important element of the defense function of the BBB. The more positive surface charge of brain endothelial cells does not influence the permeability of the paracellular pathway for hydrophilic molecules, but can restrict the permeability of lipophilic cationic molecules via the transcellular

pathway. Our observations on one hand can help to understand the biophysical background of lidocaine action, on the other hand draw attention to the drug interactions at the level of the BBB.

6. Acknowledgments
We would like to dedicate this work to our colleague Rudolf Tóth-Boconádi with whom we started this study, but who unfortunately is no longer with us.

Funding
This research work was supported by the European Training Network H2020-MSCA-ITN-2015 [Grant number 675619]; National Research, Development and Innovation Office, Hungary [grant numbers GINOP-2.3.2-15-2016-00001, OTKA K-108697, NNE 129617]; F.R.W was supported by the János Bolyai Research Fellowship of the Hungarian Academy of Sciences and the National Research, Development and Innovation Office, Hungary [grant number OTKA PD-128480].

Conflict of interest
The authors declare that they have no conflicts of interest with the contents of this article.

References
[1] Klausen LH, Fuhs T, Dong M. Mapping surface charge density of lipid bilayers by quantitative surface conductivity microscopy. Nat Commun. 2016 Aug 26;7:12447.
[2] Wojtczak L, Nałecz MJ. Surface change of biological membranes as a possible regulator of membrane-bound enzymes. Eur J Biochem. 1979 Feb 15;94(1):99-107.
[3] Seeman P. The membrane actions of anesthetics and tranquilizers. Pharmacol Rev. 1972 Dec;24(4):583-655.
[4] Sheetz MP, Singer SJ. Biological membranes as bilayer couples. A molecular mechanism of drug-erythrocyte interactions. Proc Natl Acad Sci U S A. 1974 Nov;71(11):4457-61.
[5] Baughman VL, Laurito CE, Polek WV. Lidocaine blood levels following aerosolization and intravenous administration. J Clin Anesth. 1992 Jul-Aug;4(4):325-7.
[6] Dan GA, Martinez-Rubio A, Agewall S, Boriani G, Borggrefe M, Gaita F, van Gelder I, Gorenek B, Kaski JC, Kjeldsen K, Lip GYH, Merkely B, Okumura K, Piccini JP, Potpara T, Poulsen BK, Saba M, Savelieva I, Tamargo JL, Wolpert C; ESC Scientific Document Group. Antiarrhythmic drugs-clinical use and clinical decision making: a consensus document from the European Heart Rhythm Association (EHRA) and European Society of Cardiology (ESC) Working Group on Cardiovascular Pharmacology, endorsed by the Heart Rhythm Society (HRS), Asia-Pacific Heart Rhythm Society (APHRS) and International Society of Cardiovascular Pharmacotherapy (ISCP). Europace. 2018 May 1;20(5):731-732an.
[7] Daykin H. The efficacy and safety of intravenous lidocaine for analgesia in the older adult: a literature review. Br J Pain. 2017 Feb;11(1):23-31.
[8] Tsuchiya H, Mizogami M. Interaction of local anesthetics with biomembranes consisting of phospholipids and cholesterol: mechanistic and clinical implications for anesthetic and cardiotoxic effects. Anesthesiol Res Pract. 2013;2013:297141.
[9] Weizenmann N, Huster D, Scheidt HA. Interaction of local anesthetics with lipid bilayers investigated by ^{1}H MAS NMR spectroscopy. Biochim Biophys Acta. 2012 Dec;1818(12):3010-8.

[10] Högberg CJ, Lyubartsev AP. Effect of local anesthetic lidocaine on electrostatic properties of a lipid bilayer. Biophys J. 2008 Jan 15;94(2):525-31.
[11] Katzung BG, White PF (2009). Local anesthetics. In: Katzung BG (Ed.): Basic and Clinical Pharmacology. 11th Ed. pp. 439–450. Lange Medical Books/McGraw-Hill, New York
[12] Tan JH, Saint DA. Interaction of lidocaine with the cardiac sodium channel: effects of low extracellular pH are consistent with an external blocking site. Life Sci. 2000 Oct 20;67(22):2759-66.
[13] Oesterhelt D, Stoeckenius W. Rhodopsin-like protein from the purple membrane of Halobacterium halobium. Nat New Biol. 1971 Sep 29;233(39):149-52.
[14] Kimura Y, Ikegami A, Stoeckenius W. Salt and pH-dependent changes of the purple membrane absorption spectrum. Photochem Photobiol. 1984 Nov;40(5):641-6.
[15] Renthal R, Shuler K, Regalado R. Control of bacteriorhodopsin color by chloride at low pH. Significance for the proton pump mechanism. Biochim Biophys Acta. 1990 Apr 26;1016(3):378-84.
[16] Shibata A, Yorimitsu A, Ikema H, Minami K, Ueno S, Muneyuki E, Higuti T. Photocurrent of purple membrane adsorbed onto a thin polymer film: action characteristics of the local anesthetics. Colloids Surf B Biointerfaces. 2002;23(4):375-82.
[17] Shibata A, Sakata A, Ueno S, Hori T, Minami K, Baba Y, Kamo N. Regeneration and inhibition of proton pumping activity of bacteriorhodopsin blue membrane by cationic amine anesthetics. Biochim Biophys Acta. 2005 May 15;1669(1):17-25.
[18] Abbott NJ, Patabendige AA, Dolman DE, Yusof SR, Begley DJ. Structure and function of the blood-brain barrier. Neurobiol Dis. 2010 Jan;37(1):13-25.
[19] Deli MA. Drug transport and the blood-brain barrier, in: eds K. Tihanyi and M. Vastag, Solubility, Delivery and ADME Problems of Drugs and Drug Candidates. 2011; 144–65. Washington, DC: Bentham Science Publ. Ltd.
[20] Fu BM, Tarbell JM. Mechano-sensing and transduction by endothelial surface glycocalyx: composition, structure, and function. Wiley Interdiscip Rev Syst Biol Med. 2013 May-Jun;5(3):381-90.
[21] Hervé F, Ghinea N, Scherrmann JM. CNS delivery via adsorptive transcytosis. AAPS J. 2008 Sep;10(3):455-72.
[22] Ribeiro MM, Domingues MM, Freire JM, Santos NC, Castanho MA. Translocating the blood-brain barrier using electrostatics. Front Cell Neurosci. 2012 Oct 11;6:44.
[23] Högberg CJ, Lyubartsev AP. Effect of local anesthetic lidocaine on electrostatic properties of a lipid bilayer. Biophys J. 2008 Jan 15;94(2):525-31.
[24] Matsuki H, Yamanaka M, Kamaya H, Kaneshina S, Ueda I. Dissociation equilibrium between uncharged and charged local anesthetic lidocaine in a surface-adsorbed film. Colloid and Polymer Science .2005; 283(5): 512–20.
[25] Dér A, Hargittai P, Simon J. Time-resolved photoelectric and absorption signals from oriented purple membranes immobilized in gel. J Biochem Biophys Methods. 1985 Mar;10(5-6):295-300.
[26] Khoroshyy P, Dér A, Zimányi L. Effect of Hofmeister cosolutes on the photocycle of photoactive yellow protein at moderately alkaline pH. J Photochem Photobiol B. 2013 Mar 5;120:111-9.
[27] Weksler BB, Subileau EA, Perrière N, Charneau P, Holloway K, Leveque M, Tricoire-Leignel H, Nicotra A, Bourdoulous S, Turowski P, Male DK, Roux F, Greenwood J,

Romero IA, Couraud PO. Blood-brain barrier-specific properties of a human adult brain endothelial cell line. FASEB J. 2005 Nov;19(13):1872-4.
[28] Veszelka S, Tóth A, Walter FR, Tóth AE, Gróf I, Mészáros M, Bocsik A, Hellinger É, Vastag M, Rákhely G, Deli MA. Comparison of a Rat Primary Cell-Based Blood-Brain Barrier Model With Epithelial and Brain Endothelial Cell Lines: Gene Expression and Drug Transport. Front Mol Neurosci. 2018 May 22;11:166.
[29] Nakagawa S, Deli MA, Kawaguchi H, Shimizudani T, Shimono T, Kittel A, Tanaka K, Niwa M. A new blood-brain barrier model using primary rat brain endothelial cells, pericytes and astrocytes. Neurochem Int. 2009 Mar-Apr;54(3-4):253-63.
[30] Walter FR, Veszelka S, Pásztói M, Péterfi ZA, Tóth A, Rákhely G, Cervenak L, Ábrahám CS, Deli MA. Tesmilifene modifies brain endothelial functions and opens the blood-brain/blood-glioma barrier. J Neurochem. 2015 Sep;134(6):1040-54.
[31] Perrière N, Demeuse P, Garcia E, Regina A, Debray M, Andreux JP, Couvreur P, Scherrmann JM, Temsamani J, Couraud PO, Deli MA, Roux F. Puromycin-based purification of rat brain capillary endothelial cell cultures. Effect on the expression of blood-brain barrier-specific properties. J Neurochem. 2005 Apr;93(2):279-89.
[32] Deli MA, Abrahám CS, Kataoka Y, Niwa M. Permeability studies on in vitro blood-brain barrier models: physiology, pathology, and pharmacology. Cell Mol Neurobiol. 2005 Feb;25(1):59-127.
[33] Lénárt N, Walter FR, Bocsik A, Sántha P, Tóth ME, Harazin A, Tóth AE, Vizler C, Török Z, Pilbat AM, Vígh L, Puskás LG, Sántha M, Deli MA. Cultured cells of the blood-brain barrier from apolipoprotein B-100 transgenic mice: effects of oxidized low-density lipoprotein treatment. Fluids Barriers CNS. 2015 Jul 17;12:17.
[34] Domingues MM, Santiago PS, Castanho MA, Santos NC. What can light scattering spectroscopy do for membrane-active peptide studies? J Pept Sci. 2008 Apr;14(4):394-400.
[35] Walter FR, Valkai S, Kincses A, Petneházi A, Czeller T, Veszelka S, Ormos P, Deli MA, Dér A. A versatile lab-on-a-chip tool for modeling biological barriers. Sens Actuators B Chem. 2016;222:1209-1219.
[36] Bocsik A, Walter FR, Gyebrovszki A, Fülöp L, Blasig I, Dabrowski S, Ötvös F, Tóth A, Rákhely G, Veszelka S, Vastag M, Szabó-Révész P, Deli MA. Reversible Opening of Intercellular Junctions of Intestinal Epithelial and Brain Endothelial Cells With Tight Junction Modulator Peptides. J Pharm Sci. 2016 Feb;105(2):754-765.
[37] Zimányi L, Váró G, Chang M, Ni B, Needleman R, Lanyi JK. Pathways of proton release in the bacteriorhodopsin photocycle. Biochemistry. 1992 Sep 15;31(36):8535-43.
[38] Hilal-Dandan R, Knollman B, Brunton L. Goodman and Gilman's The Pharmacological Basis of Therapeutics. McGraw-Hill Education / Medical; 12 edition, 2011.
[39] Abbott NJ, Rönnbäck L, Hansson E. Astrocyte-endothelial interactions at the blood-brain barrier. Nat Rev Neurosci. 2006 Jan;7(1):41-53.
[40] Li G, Fu BM. An electrodiffusion model for the blood-brain barrier permeability to charged molecules. J Biomech Eng. 2011 Feb;133(2):021002.
[41] Ribeiro MM, Pinto AR, Domingues MM, Serrano I, Heras M, Bardaji ER, Tavares I, Castanho MA. Chemical conjugation of the neuropeptide kyotorphin and ibuprofen enhances brain targeting and analgesia. Mol Pharm. 2011 Oct 3;8(5):1929-40.
[42] Johansson BB, Linder LE. Do nitrous oxide and lidocaine modify the blood-brain barrier in acute hypertension in the rat? Acta Anaesthesiol Scand. 1980;24(1):65-8.

[43] Beggs S, Liu XJ, Kwan C, Salter MW. Peripheral nerve injury and TRPV1-expressing primary afferent C-fibers cause opening of the blood brain barrier. Mol Pain. 2010 Nov 2;6:74.
[44] Stoeckenius W, Lozier RH, Bogomolni RA. Bacteriorhodopsin and the purple membrane of halobacteria. Biochim Biophys Acta. 1979 Mar 14;505(3-4):215-78.
[45] Yun I, Cho ES, Jang HO, Kim UK, Choi CH, Chung IK, Kim IS, Wood WG. Amphiphilic effects of local anesthetics on rotational mobility in neuronal and model membranes. Biochim Biophys Acta. 2002 Aug 19;1564(1):123-32.
[46] Ando Y, Okada H, Takemura G, Suzuki K, Takada C, Tomita H, Zaikokuji R, Hotta Y, Miyazaki N, Yano H, Muraki I, Kuroda A, Fukuda H, Kawasaki Y, Okamoto H, Kawaguchi T, Watanabe T, Doi T, Yoshida T, Ushikoshi H, Yoshida S, Ogura S. Brain-specific ultrastructure of capillary endothelial glycocalyx and its possible contribution for blood brain barrier. Sci Rep. 2018 Nov 30;8(1):17523
[47] Cereijido M, Contreras RG, Shoshani L, Flores-Benitez D, Larre I. Tight junction and polarity interaction in the transporting epithelial phenotype. Biochim Biophys Acta. 2008 Mar;1778(3):770-93.
[48] Helms HC, Abbott NJ, Burek M, Cecchelli R, Couraud PO, Deli MA, Förster C,Galla HJ, Romero IA, Shusta EV, Stebbins MJ, Vandenhaute E, Weksler B, Brodin B. In vitro models of the blood-brain barrier: An overview of commonly used brain endothelial cell culture models and guidelines for their use. J Cereb Blood Flow Metab. 2016 May;36(5):862-90.
[49] Suzuki T, Moriki Y, Goto H, Tomono K, Hanano M, Watanabe J. Investigation on the influx transport mechanism of pentazocine at the blood-brain barrier in rats using the carotid injection technique. Biol Pharm Bull. 2002 Oct;25(10):1351-5.
[50] Suzuki T, Ohmuro A, Miyata M, Furuishi T, Hidaka S, Kugawa F, Fukami T, Tomono K. Involvement of an influx transporter in the blood-brain barrier transport of naloxone. Biopharm Drug Dispos. 2010 May;31(4):243-52.
[51] Funao T, Oda Y, Tanaka K, Asada A. The P-glycoprotein inhibitor quinidine decreases the threshold for bupivacaine-induced, but not lidocaine-induced, convulsions in rats. Can J Anaesth. 2003 Oct;50(8):805-11.

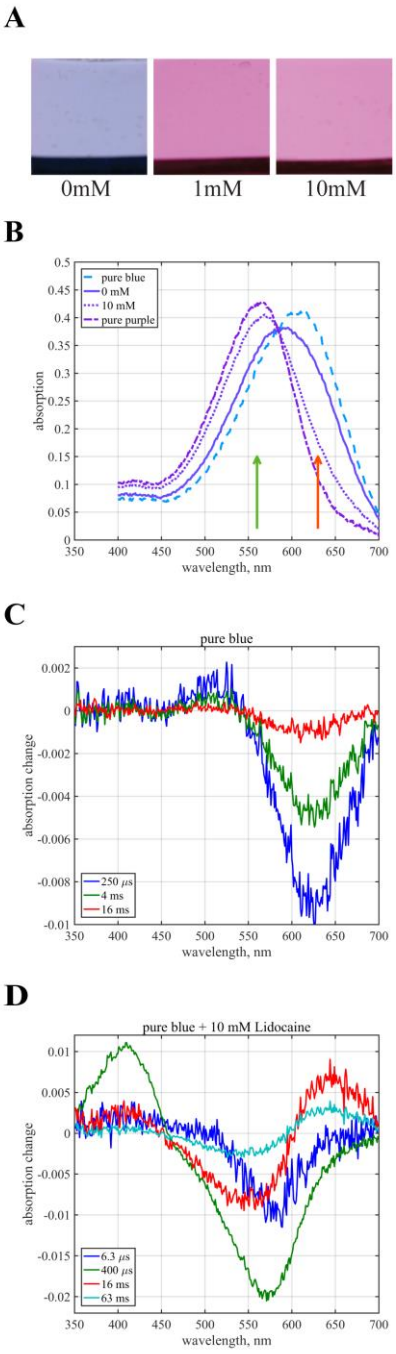

Fig. 1. Effects of lidocaine on the purple membrane. A: Photos of the gels containing purple membrane in 0.5 mM sulfuric acid (pH=3.2) without and after 1 mM and 10 mM lidocaine treatment. B: Absorption spectra of purple membrane containing gels incubated with and without lidocaine (10 mM; pH=3.0) as well as the calculated spectra for the pure purple and blue forms (see text). The arrows indicate the wavelength of the exciting laser pulses for the two samples. C, D: Time resolved difference spectra of purple membranes in polyacrylamide gel at pH 3.0, without (C) and with (D) 10 mM lidocaine.

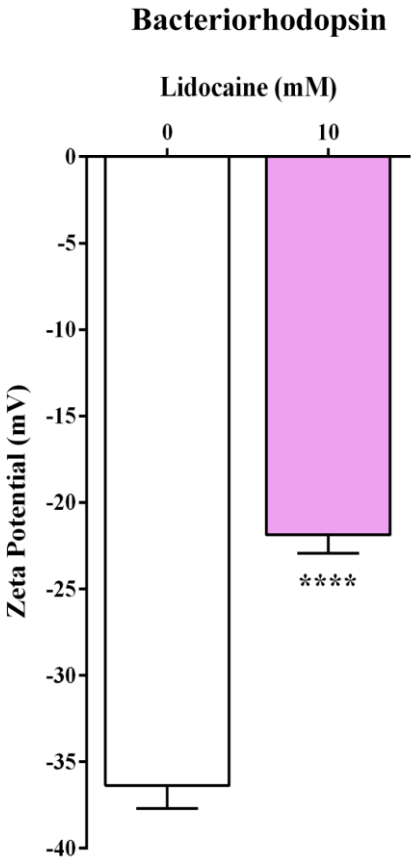

Fig. 2. Modulation of surface charge of purple membrane. Zeta potential of purple membrane in 0.5 mM H_2SO_4 (pH=3.2) without and with 10 mM lidocaine treatment (30 min). Values of each group are presented as mean ± SD, n = 10. Data were analysed by unpaired t-test. ****$p<0.0001$, compared to the untreated control.

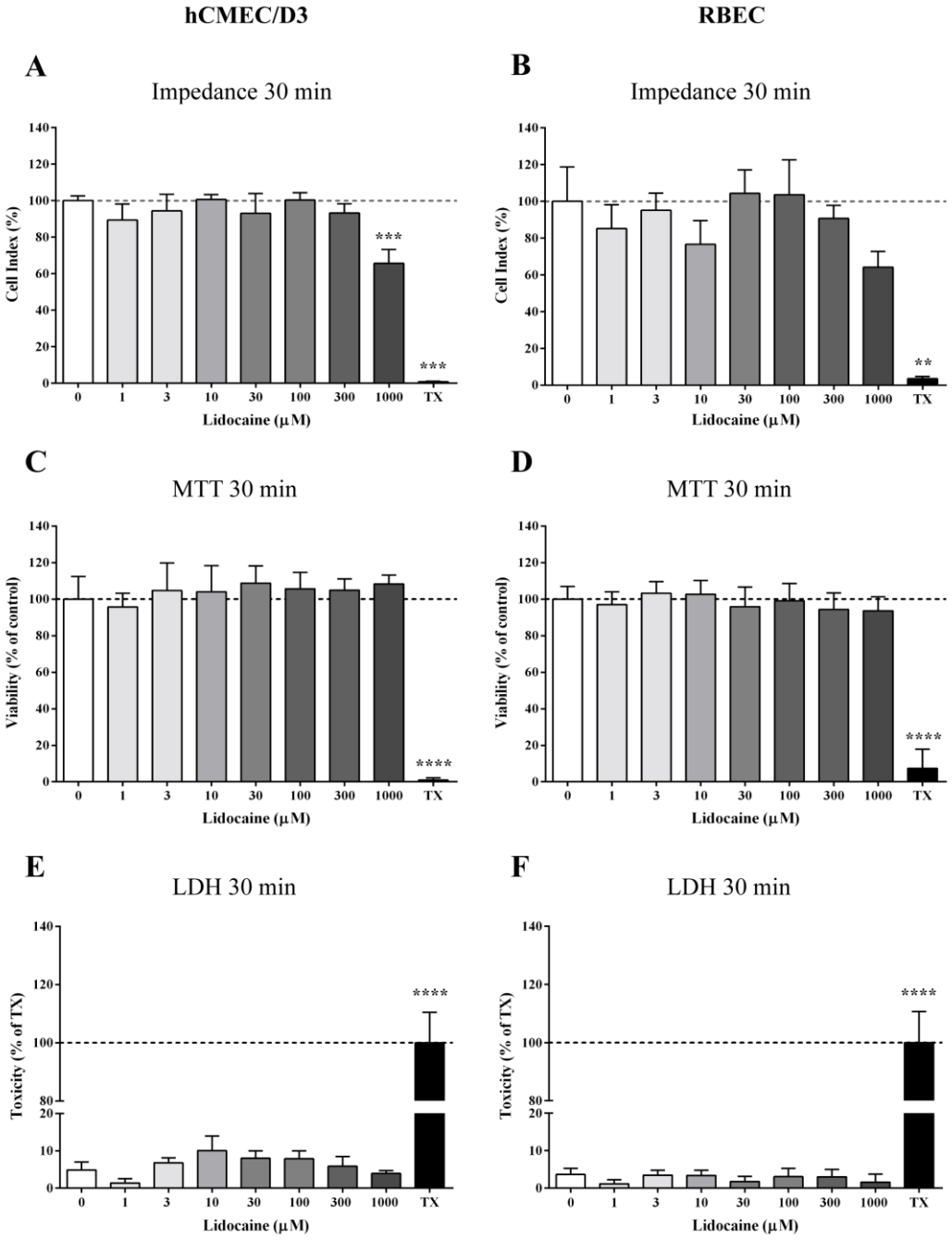

Fig. 3. Cell viability assays on the effects of lidocaine on brain endothelial cells. Treatments were performed for 30 min with concentrations of 1-1000 µM. TX: Triton X-100 detergent served as positive control. A-B: Impedance measurements on hCMEC/D3 human brain endothelial cell line and on primary rat brain endothelial cells (RBEC). C-D: The effects of lidocaine on MTT dye conversion reflecting metabolic activity. E-F: Lactate dehydrogenase (LDH) release after lidocaine treatment reflecting membrane integrity. Values of each group are presented as mean ± SD, n=6-8. Data were analysed by one-way ANOVA followed by Bonferroni post-test. ***p<0.001, ****p<0.0001 compared to the untreated control.

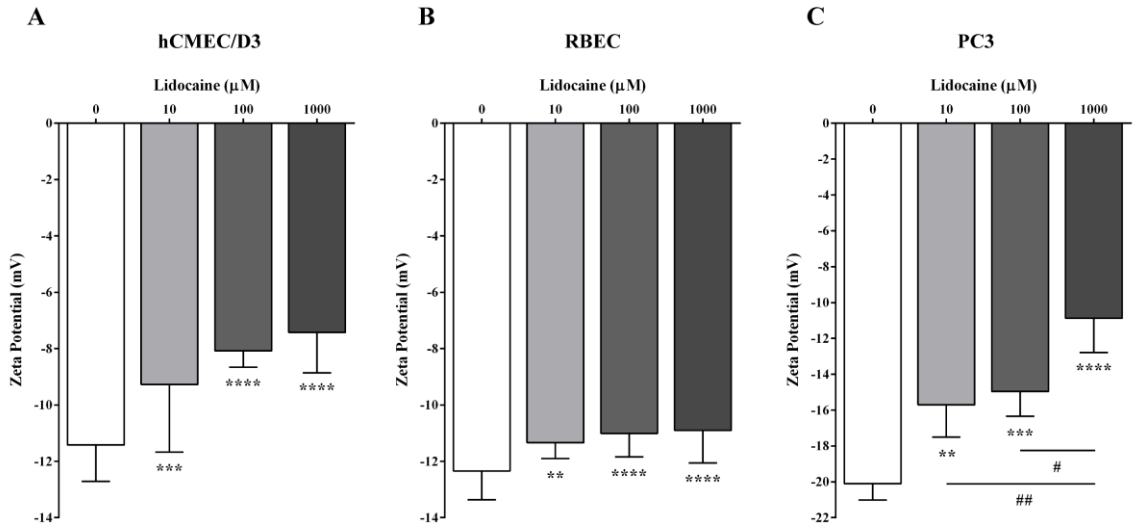

Fig. 4. Effects of lidocaine on the surface charge of living mammalian cells. Cell cultures of the human brain endothelial cell line hCMEC/D3 (A), rat primary brain endothelial cells (RBEC) (B), and human PC-3 prostate cancer cell line (C) were treated with different concentrations of lidocaine for 30 min to measure changes in the surface zeta potential. Values of each group are presented as mean ± SD, n=10-29. Data were analysed by one-way ANOVA followed by Bonferroni post-test. $^{\#}p<0.05$, **;$^{\#\#}p<0.01$, ***$p<0.001$, ****$p<0.0001$ compared to the untreated control and between treatments.

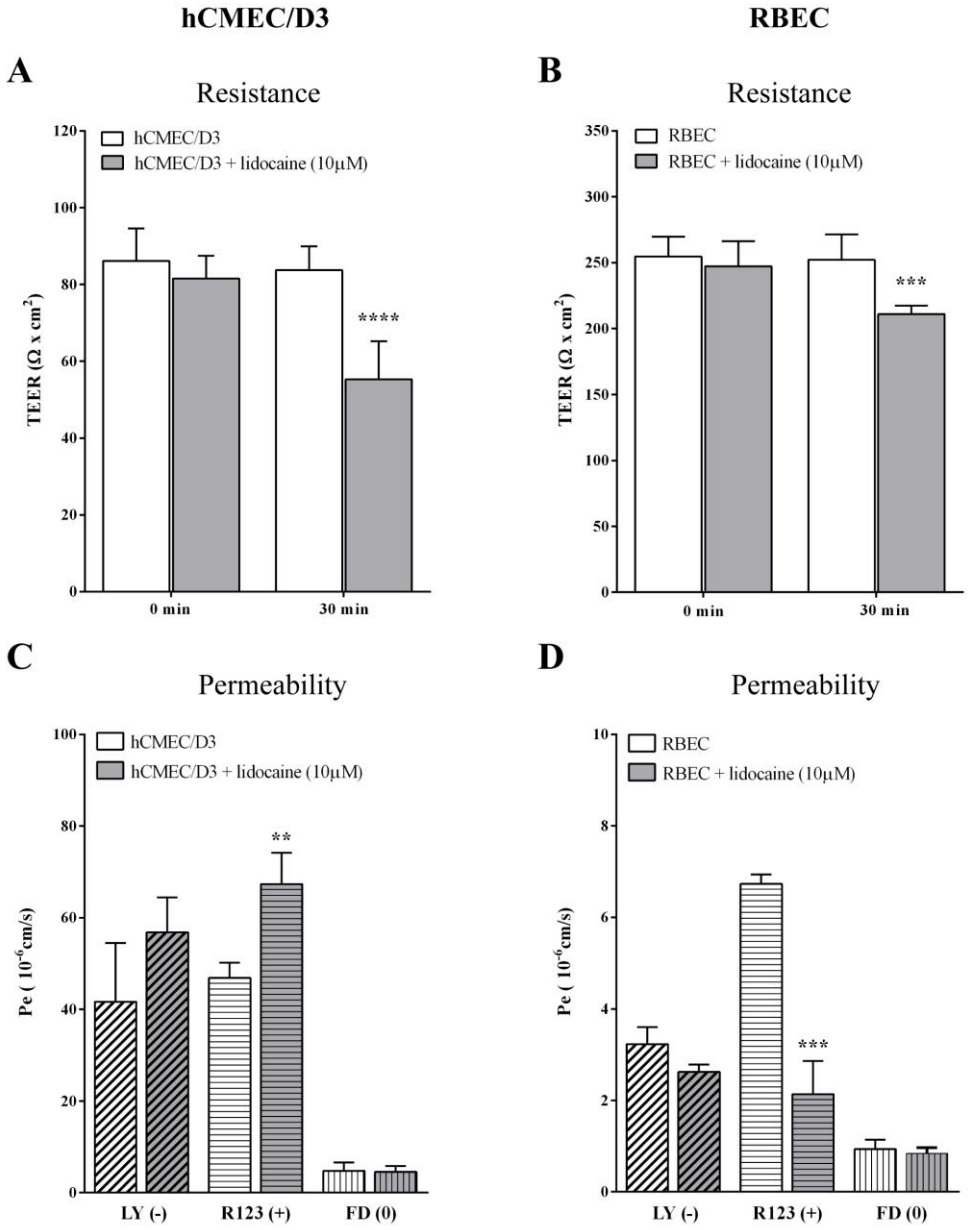

Fig. 5. Evaluation of the blood brain barrier (BBB) integrity on Transwell insert models of the BBB using hCMEC/D3 human brain endothelial cell line and rat primary cell based triple co-culture model consisting of brain endothelial cells (RBEC) with pericytes and astroglia after lidocaine treatment (10 μM, 30 min). A and B: TEER measurements right before and 30 min after the lidocaine treatment. Values of each group are presented as mean ± SD, n=5-12. Data were analysed by two-way ANOVA followed by a Bonferroni post-test. ***p<0.001, ****p<0.0001, compared to the 0 min. C and D: Endothelial permeability coefficient (P_e) of cells treated with lidocaine for three differently charged tracers: Lucifer Yellow (LY, -, negatively charged), Rhodamine 123 (R123, +, positively charged) and FITC-Dextran (FD, 0, no charge). Values are presented as mean ± SD, n=4. Data were analysed by unpaired t-test, where **p<0.01; ***p<0.001.

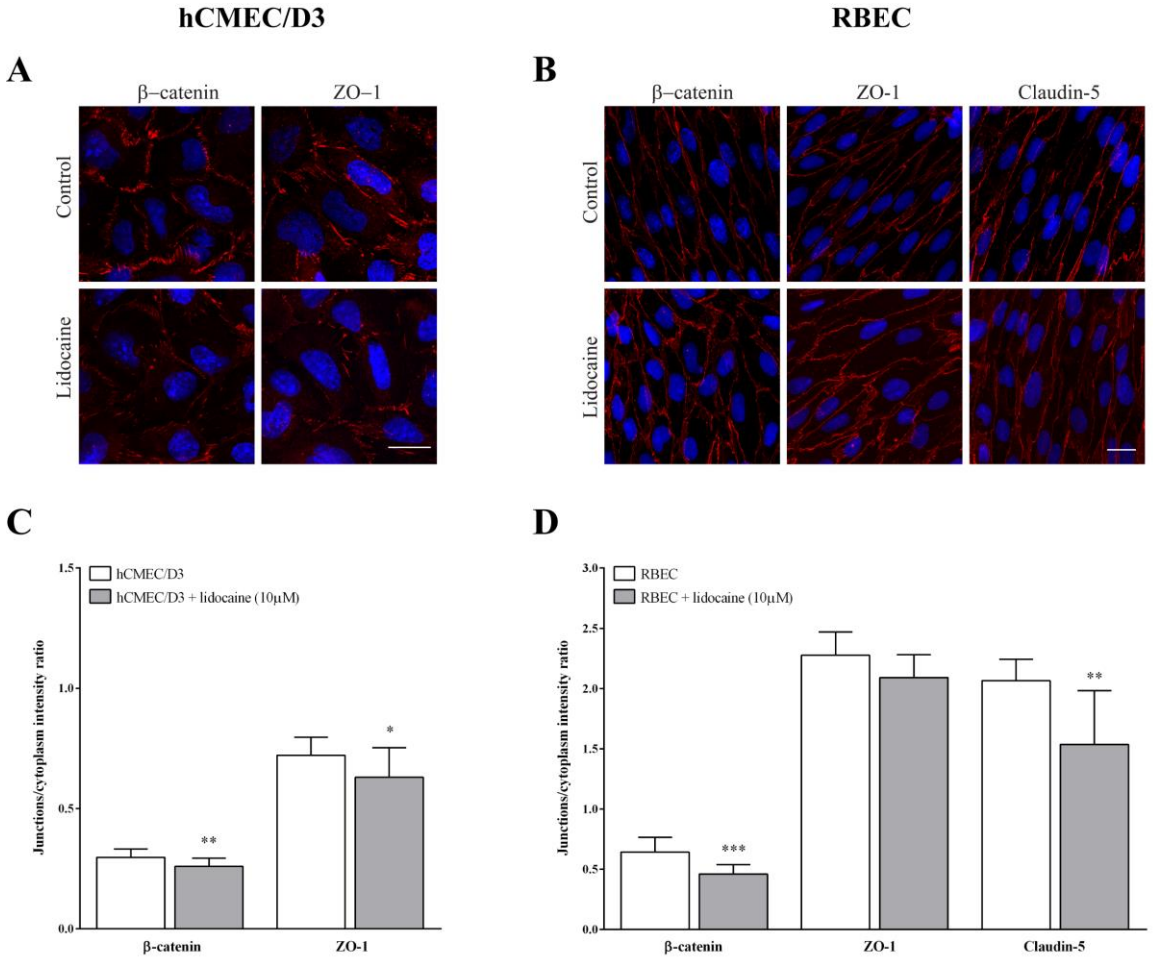

Fig. 6. A and B: Effects of lidocaine treatment (10 μM, 30 min) on β-catenin, ZO-1 and claudin-5 immunostaining in hCMEC/D3 human brain endothelial cell line and rat primary brain endothelial cells. Red: staining for junctional proteins. Blue: H33342 staining of cell nuclei. Bar: 20 μm. C and D: Intensity ratio of the junctional and the cytoplasmatic immunostainings. Values are presented as mean ± SD, n=11-15. Data were analysed by unpaired t-test. $^{*}p<0.05$, $^{**}p<0.01$, $^{***}p<0.001$, compared to the untreated control of the respective group.

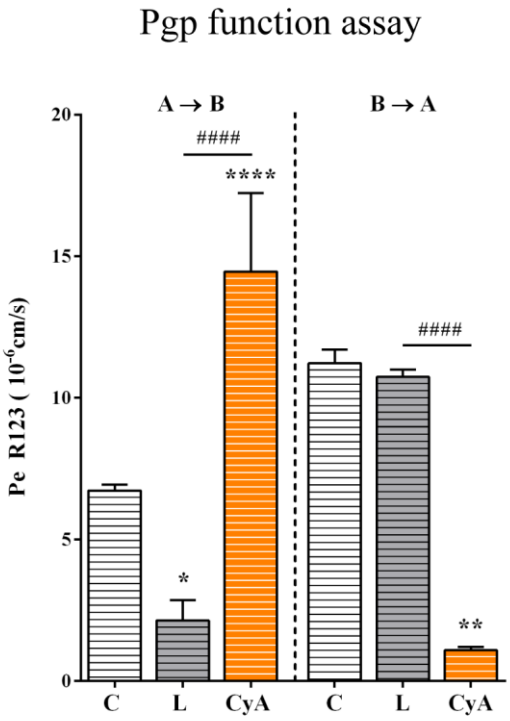

Fig. 7. Effects of lidocaine on the P-glycoprotein efflux pump activity in primary rat brain endothelial cells (RBEC). Permeability of Rhodamine 123 (R123) was measured from the abluminal to the luminal (A to B) and from the luminal to the abluminal (B to A) compartment after 30 min treatment with lidocaine or 1 hour with P-glycoprotein pump inhibitor cyclosporin-A (CyA). Values are presented as mean ± SD n=4. Data were analysed by one-way ANOVA followed by a Bonferroni post-test. *p<0.05, **p<0.01, ****, ####p<0.0001, compared to the control and between groups. C: Control, L: Lidocaine.

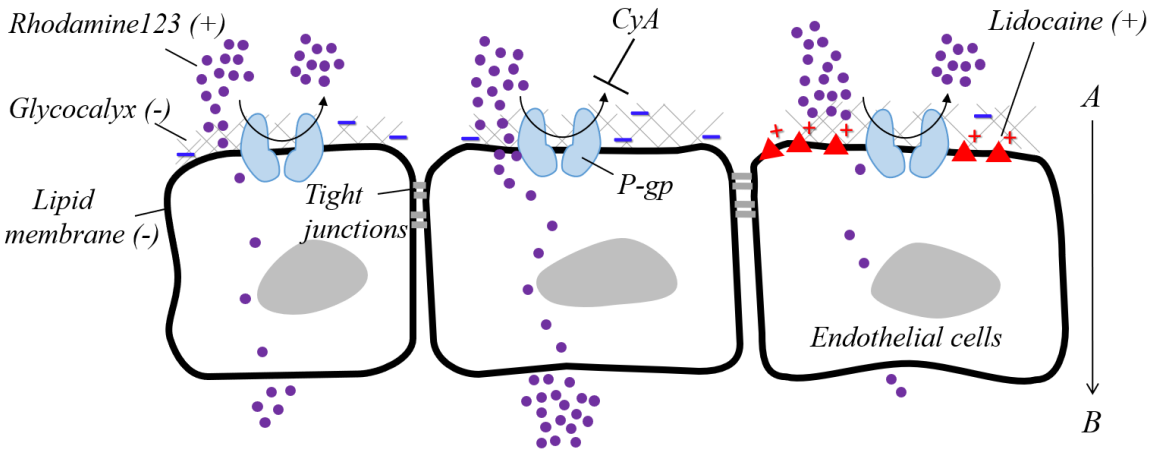

Fig. 8. A schematic figure summarizing the effects of lidocaine on cationic model molecule rhodamine 123 permeability across a tight BBB model. Rhodamine 123 under physiological conditions is pumped back to the luminal surface by the P-glycoprotein (Pgp) efflux pump, which action can be blocked by the inhibitor of the pump, cyclosporin A (CyA). Lidocaine treatment decreases the flux of rhodamine 123 through the cell layer by intercalating to the lipid bilayer and modifying the endothelial surface charge.

Supplementary Material

Supplementary Figure 1.

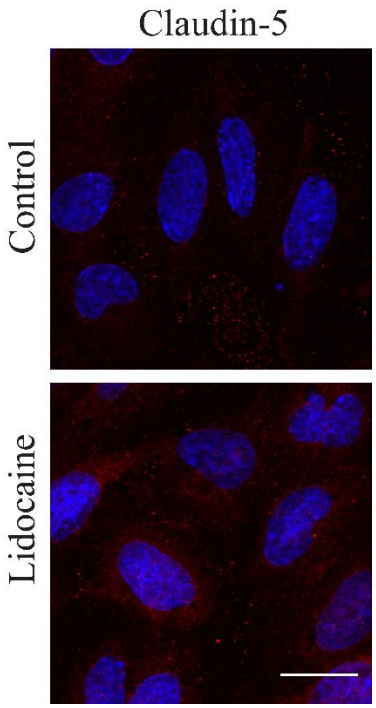

Fig. S1. Effect of lidocaine treatment (10 μM, 30 min) on TJ protein claudin-5 immunostaining in hCMEC/D3 human brain endothelial cell line. Red: staining for claudin-5. Blue: H33342 staining of cell nuclei. Bar: 20 μm.

No immunostaining is visible in the junctional area.

Supplementary Figure 2.

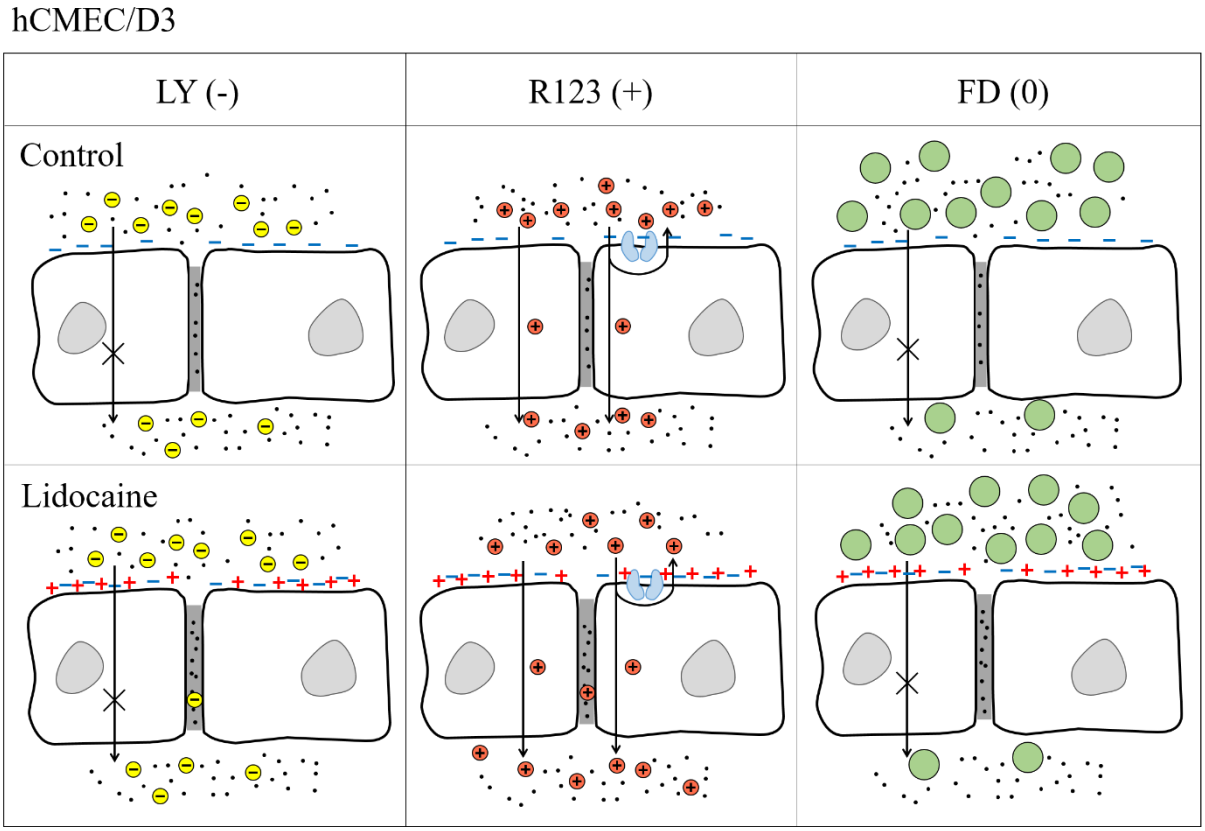

Fig S2. Drawings representing the passage of fluorescent marker molecules across the hCMEC/D3 cell culture monolayers before and after lidocaine treatment. The flux of the negatively charged marker molecule Lucifer yellow (LY, diameter ~1 nm, **yellow circles**); positively charged rhodamine 123 (R123, diameter ~1 nm, **red circles**) and neutral FITC-dextran 10 kDa (FD, diameter ~4 nm, **green circles**) are indicated. Luminal surface charge is marked by **blue lines**: indicating negative charge and **red crosses**: positive charge caused by the insertion of lidocaine; **Small dots**: Na^+ ions, diameter ~0.2 nm; **Light blue** transporter: P-glycoprotein effux pump on the luminal side. **Tight junctions** between the cells are marked by grey.

The hCMEC/D3 cell line forms a less tight barrier compared to the primary cell based BBB models (Veszelka et al., 2018, PMID 29872378). This was represented by the bigger space (grey) indicating wider intercellular clefts in the cell line model (Fig. S1) as compared to the primary BBB model (Fig. S2).
Lidocaine affected the junctional permeability as measured by TEER: the flux of sodium ions (diameter ~0.2 nm) increased across the paracellular cleft during the measurement conditions. On Fig. S1 this change is indicated by the increased thickness of the space between cells and the higher number of sodium ions (small dots) in the paracellular cleft.
The negatively charged, water soluble Lucifer yellow (LY, median axial diameter ~1 nm) crosses cell layers at the interendothelial junctions, that is the reason it is considered a paracellular permeability marker. The positive charge of the lidocaine in the cell membrane is not changing the transcellular passage, because for a hydrophilic molecule this is

negligible. The change in the junctional tightness is enough in the case of the small sodium ion to be detected, but for the 5-times larger LY, we can only see a trend for a higher transfer. A negligible transmembrane and restricted paracellular passage is true for the neutral marker FITC-dextran with a diameter of 4 nm, 20-times bigger than that of sodium ions, resulting in no change in the transfer of the molecule even after lidocaine treatment.
In the case of the positively charged and lipophilic rhodamine 123 (diameter ~1 nm), there are three pathways influencing its passage: it can cross both the paracellular and transcellular routes, and in addition the P-glycoprotein efflux pump pumps back the marker to the luminal side. The hCMEC/D3 cell line expresses less Pgp than the primary BBB model (Veszelka et al., 2018, PMID 29872378). We hypothesize that the two main factors in the increased R123 flux across the cell layers are the wider tight junctions and the lower pumping efficiency of the Pgp, which is highly dependent on cell polarization caused by junctional tightness. This effect cannot be balanced by the more positive surface charge in the hCMEC/D3 cell membrane.

Supplementary Figure 3.

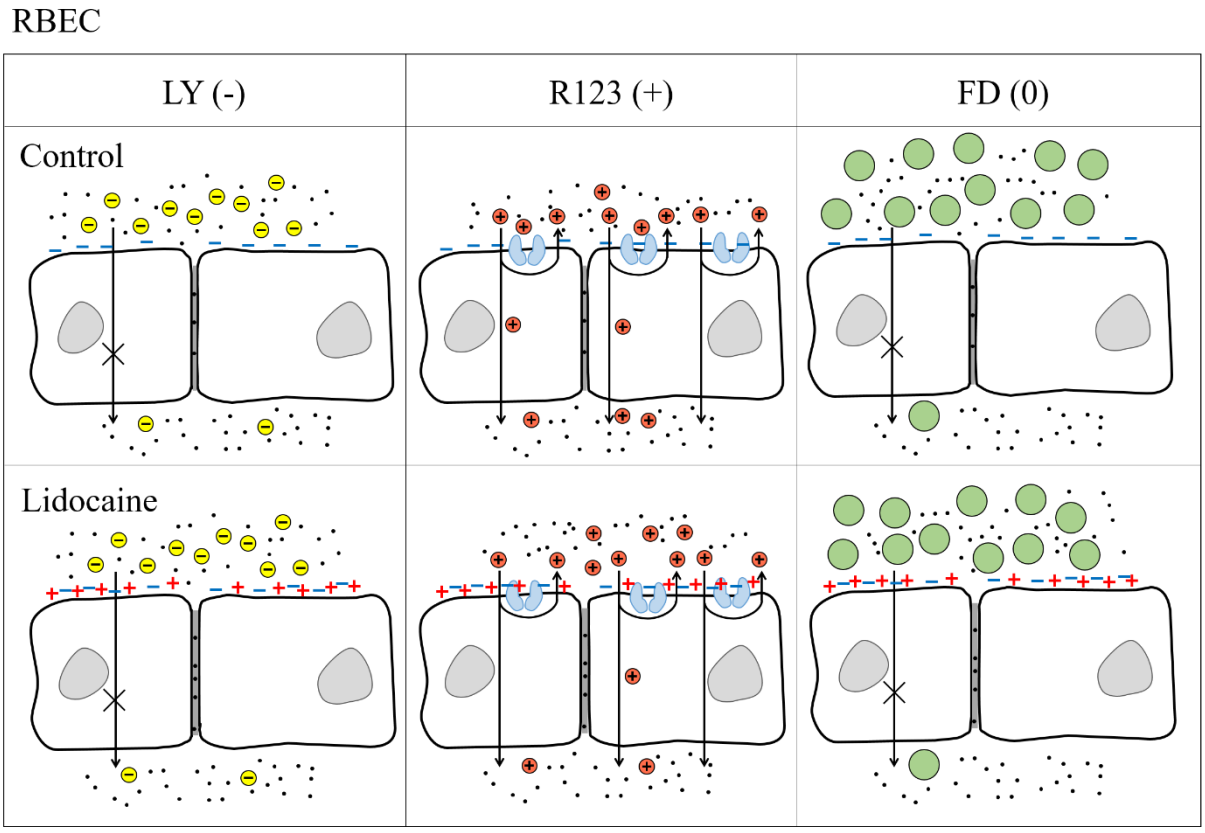

Fig S3. Drawings representing the passage of fluorescent marker molecules across primary rat brain endothelial model (RBEC) before and after lidocaine treatment. The flux of the negatively charged marker molecule Lucifer yellow (LY, diameter ~1 nm, **yellow circles**); positively charged rhodamine 123 (R123, diameter ~1 nm, **red circles**) and neutral FITC-dextran 10 kDa (FD, diameter ~4 nm, **green circles**) are indicated. Luminal surface charge is marked by **blue lines**: indicating negative charge and **red crosses**: positive charge caused by the insertion of lidocaine; **Small dots**: Na^+ ions,

diameter ~0.2 nm; **Light blue** transporter: P-glycoprotein effux pump on the luminal side. **Tight junctions** between the cells are marked by grey.

The primary BBB model forms a tighter paracellular barrier than the hCMEC/D3 cells (Veszelka et al., 2018, PMID 29872378) as indicated by the higher TEER and lower permeability values for all the marker molecules. This was represented by the smaller space (grey) between cells indicating narrower intercellular clefts in the BBB model (Fig. S2) as compared to the cell line model (Fig. S1).
The passage of the negatively charged, water soluble Lucifer yellow (LY, diameter ~1 nm) across the interendothelial junctional space is more restricted than in the case of the cell line. The positive charge of the lidocaine in the cell membrane does not change the transcellular passage, because for a hydrophilic molecule this is negligible. The change in the junctional tightness is enough to detect a higher sodium ion flux, but in the case of LY, with a 5-times bigger diameter, no change is seen. In the case of the neutral marker FITC-dextran (diameter: 4 nm, 20-times bigger than that of sodium ions) a negligible transmembrane and a restricted paracellular passage result in unchanged flux of the molecule even after lidocaine treatment. In the primary BBB model two from the three pathways influencing R123 flux is different as compared to the cell line model: the paracellular route is more restricted due to the tighter junctions, and the P-glycoprotein efflux pump expression and activity are also higher (Veszelka et al., 2018, PMID 29872378). As a result, in the control condition the R123 passage across the BBB model is much lower than in the hCMEC/D3 model. Lidocaine alters the junctional cleft as measured by the increased sodium ion flux during TEER measurement, but we hypothesize that this change is not enough to increase the paracellular R123 passage based on data with LY which has a similar molecular diameter. With the Pgp pumps actively working in the BBB model, as shown by the vectorial transfer of R123, from the three pathways it is the transmembrane flux that is changed most by lidocaine. In the presence of a restricted paracellular flux and active efflux, the more positive surface charge in the membrane caused by lidocaine results in a decreased transfer of R123 due to physicochemical interference.